

Novel Wholly Aromatic Sulfonated Poly(arylene ether) Copolymers Containing Sulfonic Acid Groups on the Pendants for Proton Exchange Membrane Materials

Jinhui Pang, Haibo Zhang, Xuefeng Li, and Zhenhua Jiang*

Alan G. MacDiarmid Institute, Department of Chemistry, Jilin University, Qianjin Street 2699, Changchun 130012, People's Republic of China

Received January 11, 2007; Revised Manuscript Received October 4, 2007

ABSTRACT: A series of novel wholly aromatic sulfonated poly(arylene ether) copolymers containing sulfonic acid groups on the pendants [SC-SPAE, i.e., side-chain-type sulfonated poly(arylene ether)] were prepared by direct copolymerization of sulfonated monomer [sodium 4-(4-(2,6-difluorobenzoyl)phenoxy) benzenesulfonate (SDFBS)], 4,4'-dichlorodiphenyl sulfone (DCDPS), and 4,4'-dihydroxydiphenylether (DHDPE). The sulfonate degree (DS) of the copolymers was readily controlled by adjusting the feed ratio of SDFBS to DCDPS. Structures of the sulfonated copolymers were confirmed by FT-IR and NMR. Tough and flexible films of the wholly aromatic copolymers with good thermal and oxidative stability were obtained by solvent cast process in *N,N*-dimethylacetamide (DMAc) solution. The films of these side-chain-type copolymers show good dimensional stability, and their water uptake and swelling ratios at high temperature are lower than those of the main-chain-type sulfonated poly(arylene ether) with similar ion exchange capacity (IEC) value. Proton conductivities of the copolymers with high sulfonate degree (DS > 0.7) are higher than 10^{-2} S/cm and increase gradually with increasing temperature. At 100 °C, the conductivities of SC-SPAE90 (DS = 0.9, IEC = 1.61 mmol g⁻¹) and SC-SPAE100 (DS = 1.0, IEC = 1.74 mmol g⁻¹) reach 0.12 and 0.14 S/cm, respectively, comparable to that of Nafion117 (0.14 S/cm).

Introduction

Over the past decade, proton-conducting polymers have attracted extensive attention due to their application potential as a proton exchange membrane (PEM), which functions as an electrolyte to transfer protons from the anode to the cathode and provide a barrier for electrons, fuel, and oxygen cross-leaks between the electrodes in a proton exchange membrane fuel cell (PEMFC).^{1–4} At present, perfluorosulfonic acid PEMs, such as Dupont's Nafion, are typically used as the polymer electrolytes in PEMFC due to their excellent chemical and mechanical stabilities as well as high proton conductivity. However, the practical applications of the perfluorosulfonic acid PEMs in large scale are limited to some extent due to their high methanol permeability, low conductivity at high temperature, and high cost. Recently, great efforts have been made to design and synthesize alternative PEM materials of the perfluorosulfonic acid. Among the alternative materials investigated, sulfonated aromatic polymers, such as sulfonated poly(arylene ether ketone),^{5–7} sulfonated poly(arylene ether sulfone),⁸ sulfonated polyimides,⁹ sulfonated poly(arylene ether nitrile),^{10,11} and sulfonated poly(benzimidazole),¹² have been considered as promising candidates as alternative PEM materials due to their high thermal and chemical stability, high proton conductivity, and low cost. Usually the sulfonated aromatic polymers can be obtained by either post-sulfonation of the aromatic polymers or direct copolymerization of the sulfonated monomer. As compared to the post-sulfonation, the direct copolymerization allows close control of sulfonate content in the polymers and is effective to suppress the possible cross-linking or other side reactions that may occur during the post-sulfonation process.^{13–15}

The sulfonated aromatic polymers can be divided into two types according to the position of the sulfonic acid groups

attached, main-chain-type¹⁵ and side-chain-type,^{19–27} in which the sulfonic acid groups are attached to the polymer backbone and side chains, respectively. Ionomers with sulfonic acid groups attached directly to their backbone usually show an intensive water uptake over a critical temperature or sulfonate degree, resulting in unfavorable excess water swelling of the membranes.¹⁶ A strategy to lower the water swelling ratio is to distinctly separate the hydrophilic sulfonic acid groups from the hydrophobic polymer main chain.^{17,18} For side-chain-type sulfonated polymers, the existence of short pendent side chains between the polymer main chain and the sulfonic acid groups is meaningful for the nanophase separation of hydrophilic and hydrophobic domains, and improved hydrolytic stability of the ionomer membranes.^{19,20} A variety of side-chain-type sulfonated polymers have been prepared by chemical grafting method or by post-sulfonation on the activated pendants of the corresponding parent polymers,²¹ including benzylsulfonated substituted poly(benzimidazole),²² polysulfone with sulfonated aromatic side chains, and the sulfonated derivatives of poly(*p*-phenylene).²³ Kobayashi et al. found that sulfonated poly(4-phenoxybenzoyl-1,4-phenylene) (SPPBP) with pendant side chain between polymer main chain and sulfonic acid groups by post-sulfonation reaction of corresponding parent polymers showed higher and more stable proton conductivity.²⁴ Ghassenmia et al. synthesized novel side-chain-type sulfonated poly(*p*-phenylene) derivatives with proton conductivity in the range of 0.06–0.11 S/cm.^{23,25} Jannasch et al. prepared side-chain-type sulfonated polysulfones via lithiation of polysulfone and anionic reaction with sulfobenzoic acid cyclic anhydride.²⁸ In addition, some side-chain-type sulfonated polyimides (SPI)^{29,30} with higher proton conductivity and better water stability than the main-chain-type ones have been prepared from novel sulfonated diamine monomer by direct copolymerization. As compared to chemical grafting and post-

* Corresponding author. E-mail: jiangzhenhua@jlu.edu.cn.

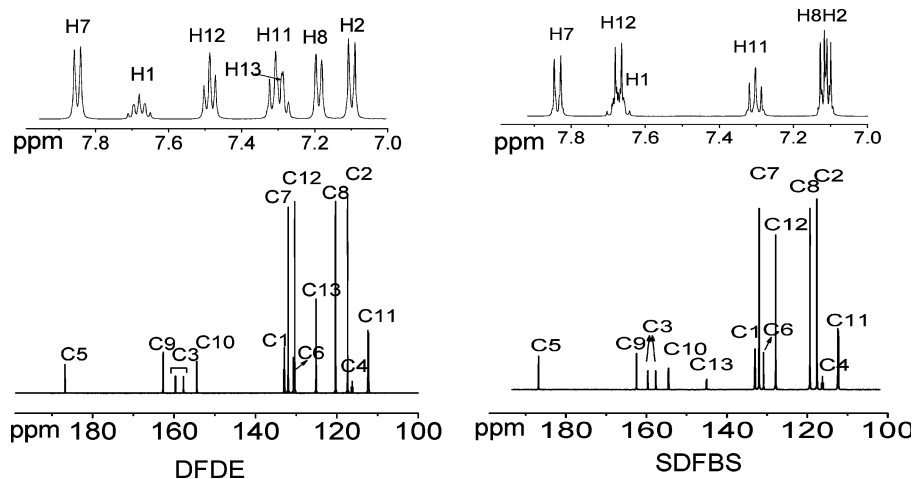
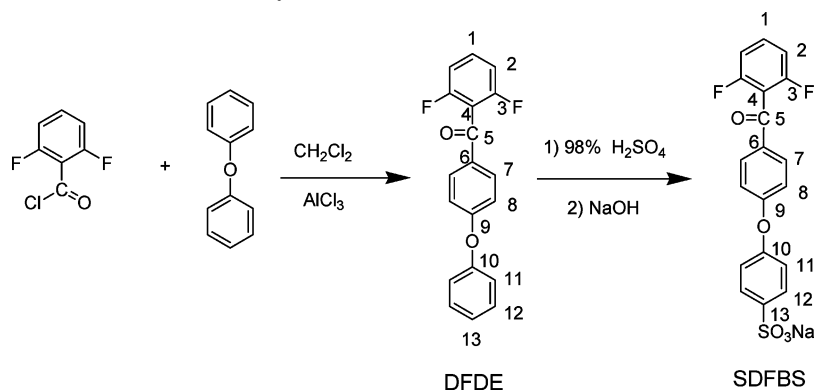


Figure 1. ^1H NMR and ^{13}C NMR spectra of the monomers DFDE and SDFBS (see Scheme 1 for labels).

Scheme 1. Synthesis of Sulfonated Monomer SDFBS



sulfonation methods, direct copolymerization method allows close control of the polymer structure.

In this Article, we synthesized sulfonated monomer sodium-4-(4-(2,6-difluorobenzoyl)phenoxy) benzenesulfonate (SDFBS) and prepared the corresponding side-chain-type sulfonated poly(arylene ether)s with various sulfonate degree by the direct copolymerization method. The properties of these novel sulfonated copolymers, such as thermal property, water uptake, water swelling ratio, and proton conductivity, were also investigated.

Experimental Section

Materials. 2,6-Difluorobenzoyl chloride and 4,4'-dihydroxydiphenylether (DHDPE) were purchased from Aldrich. Diphenyl ether (DPE) and 4,4'-dichlorodiphenyl sulfone were purchased from Shanghai Chemical Factory. Other chemical reagents and the organic solvents were purchased from Beijing Chemical Reagent and were purified by conventional methods. K_2CO_3 was dried at $120\text{ }^\circ\text{C}$ for 24 h before used.

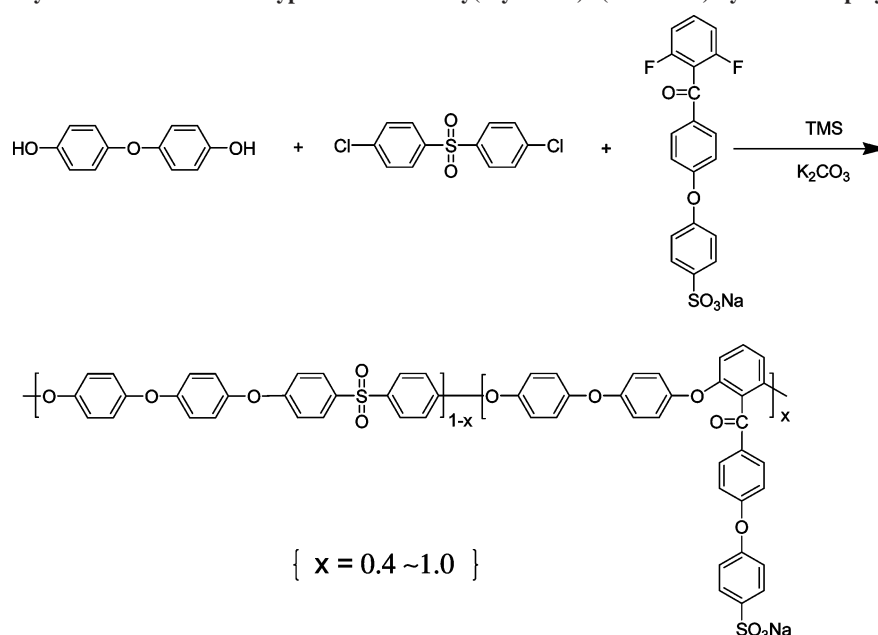
Synthesis of 4-(2,6-Difluorobenzoyl)diphenyl Ether (DFDE). A 250 mL three-neck flask equipped with a mechanical stirrer, a dropping funnel, and a nitrogen inlet was charged with diphenyl ether (18.7 g, 0.11 mol) and CH_2Cl_2 (75 mL). The solution was cooled to $0\text{ }^\circ\text{C}$, and anhydrous AlCl_3 (14.6 g, 0.11 mol) was added in several portions. After the solution was stirred for 10 min, 2,6-difluorobenzoyl chloride (17.6 g, 0.1 mol) was added dropwise over 10 min. The solution was stirred at $0\text{ }^\circ\text{C}$ for 4 h and poured into 100 mL of 1 M hydrochloric acid ice-water solution. The organic phase was separated and washed with 10% NaOH (1 \times 100 mL) and H_2O (4 \times 100 mL). The solution was dried with anhydrous MgSO_4 , and the solvent was evaporated in vacuum. After being recrystallized in petroleum (60– $90\text{ }^\circ\text{C}$) and dried, 28.5 g of white crystals was obtained. Yield: 92%. Mp (DSC): $81\text{ }^\circ\text{C}$. The ^1H

NMR and ^{13}C NMR spectra were measured in $\text{DMSO}-d_6$. ^1H NMR: 7.09 (d, $J = 8.8\text{ Hz}$, 2H, H_2); 7.18 (d, $J = 8.9\text{ Hz}$, 2H, H_8); 7.29 (t, $J = 7.5\text{ Hz}$, 1H, H_{13}); 7.30 (t, $J = 8.1\text{ Hz}$, 2H, H_{11}); 7.49 (t, $J = 8.0\text{ Hz}$, 2H, H_{12}); 7.68 (m, 1H, H_1); 7.84 (d, $J = 8.7\text{ Hz}$, 2H, H_7). ^{13}C NMR: 112.30 (2C, C_{11}); 116.24 (1C, C_4); 117.35 (2C, C_2); 120.30 (2C, C_8); 125.12 (1C, C_{13}); 130.35 (2C, C_{12}); 130.69 (1C, C_6); 131.97 (2C, C_7); 132.91 (1C, C_1); 154.40 (2C, C_{10}); 157.69, 159.63 (2C, C_3); 162.71 (1C, C_9); 186.79 (1C, C_5).

Synthesis of Sodium-4-(4-(2,6-difluorobenzoyl)phenoxy)benzenesulfonate (SDFBS). DFDE (31 g, 0.1 mol) was dissolved in 50 mL of concentrated sulfuric acid (98%). The red solution was stirred at $80\text{ }^\circ\text{C}$ for 6 h, then cooled to room temperature and poured into 120 mL of ice water. The resulting buff precipitate was filtered and dissolved in 100 mL of 10% NaOH aqueous solution. The mixture was cooled to room temperature, and the white precipitate was filtered and dried. After being recrystallized from water and dried in a vacuum oven at $120\text{ }^\circ\text{C}$ for 24 h, 37.0 g of white needles was obtained. Yield: 90%. The ^1H NMR and ^{13}C NMR spectra were measured in $\text{DMSO}-d_6$. ^1H NMR: 7.10 (d, $J = 8.6\text{ Hz}$, 2H, H_2); 7.11 (d, $J = 8.9\text{ Hz}$, 2H, H_8); 7.30 (t, $J = 8.1\text{ Hz}$, 2H, H_{11}); 7.66 (d, $J = 8.6\text{ Hz}$, 2H, H_{12}); 7.67 (m, 1H, H_1); 7.83 (d, $J = 8.8\text{ Hz}$, 2H, H_7). ^{13}C NMR: 112.37 (2C, C_{11}); 116.20 (1C, C_4); 117.59 (2C, C_2); 119.31 (2C, C_8); 127.84 (2C, C_{12}); 130.87 (1C, C_6); 131.96 (2C, C_7); 132.98 (1C, C_1); 144.99 (1C, C_{13}); 154.51 (2C, C_{10}); 157.64, 159.62 (2C, C_3); 162.47 (1C, C_9); 186.83 (1C, C_5).

Synthesis of Side-Chain-Type Sulfonated Poly(arylene ether) Copolymers (SC-SPAE). A typical synthesis procedure of SC-SPAE60, where 60 refers to the feed percent of SDFBS, was as follows. A 100 mL three-neck round-bottomed flask equipped with a nitrogen inlet and a dropping funnel was charged with SDFBS (4.944 g, 0.012 mol), DCDPS (2.296 g, 0.008 mol), DHDPE (4.040 g, 0.02 mol), potassium carbonate (3.080 g, 0.022 mol), toluene (10 mL), and tetramethylene sulfone (TMS, 40 mL). The mixture was kept at room temperature for a few minutes and

Scheme 2. Synthesis of Side-Chain-Type Sulfonated Poly(aryl ether)s (SC-SPAE) by Direct Copolymerization



then heated at 140 °C for 3 h and at 180 °C for 6 h in nitrogen atmosphere under magnetic stirring. After the reaction, 15 mL of TMS was added into the mixture to lower the solution viscosity. The solution was poured into 100 mL of toluene, and the product was obtained as white flakes. After being washed with hot deionized water and methanol alternatively several times, treated in a Soxhlet extractor with alcohol under reflux, and dried in vacuo at 80 °C for 15 h, 9.3 g of pure SC-SPAE60 was obtained. Yield: 91%.

Analysis and Measurements of the Copolymers. The viscosities of the obtained copolymers were determined by using a Ubbelohde viscometer in thermostatic container with the polymer concentration of 0.5 g/dL in DMAc at 25 °C. FTIR spectra (film) were measured on a Nicolet Impact 410 Fourier-transform infrared spectrometer. ¹H NMR and ¹³C NMR experiments were carried out on a Bruker 510 spectrometer (¹H, 500 MHz, ¹³C, 125 MHz) by using DMSO-*d*₆ as solvent.

Film Formation and Proton Exchange. Sodium-form SC-SPAE (SC-SPAE-Na) copolymer (1.0 g) was dissolved in DMAc (10 mL) overnight. Next, the solution was filtered with a fine glass frit filter funnel and cast directly onto clean glass plates. After being carefully dried at 60 °C for 10 h and vacuum-dried at 120 °C for 24 h, tough and flexible films of SC-SPAE-Na were obtained. The membranes were transformed to the acid forms (SC-SPAE-H) by proton exchange in 1 M H₂SO₄ for 24 h at room temperature. Next, the membranes were soaked and washed thoroughly with deionized water. The thickness of membranes was in the range of 60–80 μm.

Thermal Properties of the Membranes. Differential scanning calorimeter (DSC) measurements were performed on a Mettler Toledo DSC821^e instrument at a heating rate of 10 °C/min from 50 to 300 °C under nitrogen. The glass-transition temperatures (*T*_g) of the membranes were reported as the midpoint of the step transition in the second heating run. Thermogravimetric analysis (TGA) on a Perkin Elmer Pyris 1 thermal analyzer system was employed to assess thermal stability of the membranes. Before the analysis, the membranes were dried and kept in the TGA furnace at 120 °C under an air atmosphere for 30 min to remove water. The samples were evaluated in the range of 100–800 °C at a heating rate of 10 °C/min in air.

Ion Exchange Capacity. The ion exchange capacity (IEC) values of the membranes were determined by acid–base titration. Pieces of the membranes were immersed in 2 M NaCl solution for 72 h. The solution was then titrated with a 5 mM NaOH aqueous solution using phenolphthalein as indicator. The IEC values were calculated

from the titration results as the ratio of the amount of NaOH consumed (mmol) to the weight of the dried membrane samples (g).

Water Uptake and Swelling Ratio Measurements. The membranes were soaked in deionized water to reach equilibrium at the desired temperature. The membranes were then dried at 120 °C for 24 h. Weights or lengths of the dry and wet membranes were measured. The water uptake content was calculated by

$$\text{water uptake (\%)} = [(W_{\text{wet}} - W_{\text{dry}})/W_{\text{dry}}] \times 100\%$$

where *W*_{dry} and *W*_{wet} are the weights of the dried and wet samples, respectively. The swelling ratio was calculated from the change of film length by

$$\text{swelling ratio (\%)} = [(l_{\text{wet}} - l_{\text{dry}})/l_{\text{dry}}] \times 100\%$$

where *l*_{wet} and *l*_{dry} are the lengths of the wet and dry membranes, respectively.

Oxidative and Hydrolytic Stability. A small piece of the membrane sample was soaked in Fenton's reagent (3% H₂O₂ containing 2 ppm FeSO₄) at 80 °C. The oxidative stability was evaluated by recording the time when the membranes began to dissolve and disappeared.

Proton Conductivity and Methanol Permeability. Proton conductivity measurements were conducted on a Solatron-1260/1287 impedance analyzer over a frequency range of 10–10⁷ Hz with 50–500 mV oscillating voltage. A sheet of the sulfonated membrane (15 mm × 10 mm) was placed in a test cell.^{15a} Before the measurements, the membranes were fully hydrated in water at different temperatures for 48 h. The impedance measurements were performed in water vapor with 100% relative humidity (RH) at the desired temperature. The conductivity (σ) of the membranes in the transverse direction was calculated from the following equation:

$$\sigma = D/(LBR)$$

where *D* is the distance between the two electrodes, and *L* and *B* are the thickness and width of the film samples, respectively.

The methanol diffusion coefficient was determined by using a cell basically consisting of two-half-cells separated by the membrane, which was fixed between two rubber rings. Methanol 15 mol/L was placed on one side of the diffusion cell, and water was placed on the other side. Magnetic stirrers were used on each compartment to ensure uniformity. The concentration of the

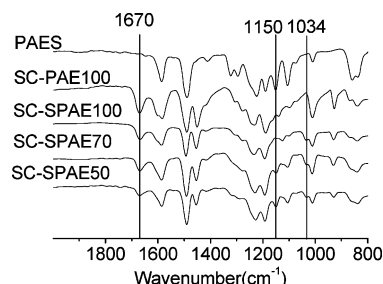


Figure 2. FT-IR spectra of SC-SPAEs, SC-PAE100, and PAES.

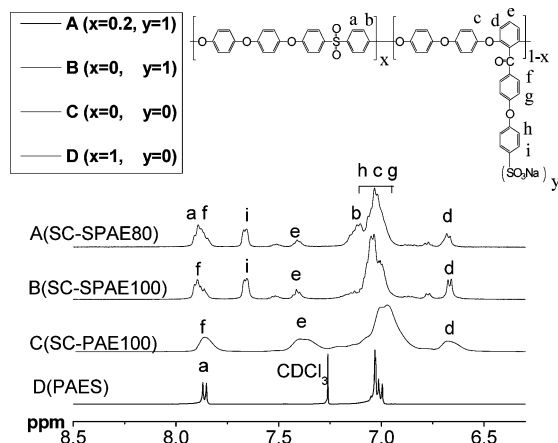


Figure 3. ^1H NMR spectra of SC-SPAEs, SC-PAE100, and PAES.

Table 1. Composition and Properties of SC-SPAEs

polymer	x	DS	IEC ^a	IEC ^b	η_{inh} (dL/g)	methanol permeability (cm ² /s)
SC-SPAE100	1.0	1.0	1.81	1.74	1.90	3.28×10^{-7}
SC-SPAE90	0.9	0.9	1.67	1.61	2.14	2.87×10^{-7}
SC-SPAE80	0.8	0.8	1.52	1.50	2.13	1.63×10^{-7}
SC-SPAE70	0.7	0.7	1.37	1.36	2.32	3.48×10^{-8}
SC-SPAE60	0.6	0.6	1.20	1.22	2.36	1.86×10^{-8}
SC-SPAE50	0.5	0.5	1.03	0.96	1.76	3.18×10^{-9}
SC-SPAE40	0.4	0.4	0.85	0.80	2.48	$<10^{-9}$

^a Theoretical value (mmol g⁻¹). ^b Experimental value (mmol g⁻¹).

methanol was measured by using a SHIMADU GC-8A chromatograph. Peak areas were converted into methanol concentration with a calibration curve. The methanol diffusion coefficient was calculated according to ref 31.

Mechanical Properties. Mechanical properties of the thin dry and wet films were evaluated at room temperature on SHIMADU AG-I 1KN at a strain rate of 10 mm/min, and a 500 N load cell was used. The samples were prepared by being cut into a dumbbell shape. The samples in the wet state were obtained by immersing the samples in water for 48 h, and the samples in the dry state were obtained by putting the samples in a vacuum oven at 60 °C for 10 h.

Atomic Force Microscopic (AFM) Observations. Tapping mode AFM observations were performed with a Digital Dimension 3000 Instrument, using micro-fabricated cantilevers with a force constant of approximately 40 N/m. The ratio of amplitudes used in feedback control was adjusted to 0.6 of the free air amplitude for all of the reported images. All samples were measured under relative humidity of 30%.

Results and Discussion

Synthesis and Characterization of the Sulfonated Monomer and Sulfonated Poly(arylene ether). The two-step synthetic route for the sulfonate monomer SDFBS is shown in Scheme 1. DFDE was first prepared by an aluminum chloride anhydrous-catalyzed Friedel–Crafts acylation of diphenylether with 2,6-difluorobenzoyl chloride and subsequently sulfonated

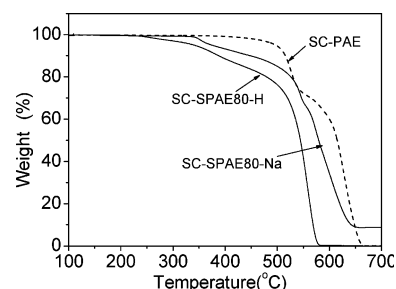


Figure 4. Typical TGA curves of SC-SPAE80 and SC-PAE in air.

Table 2. Thermal Properties of SC-SPAEs

polymer	T_g (°C)	T_d (°C) (5%)		T_d (°C) (10%)	
		acid	sodium	acid	sodium
SC-SPAE100	254	339	368	385	440
SC-SPAE90	248	345	371	385	441
SC-SPAE80	243	345	379	386	441
SC-SPAE70	231	346	376	435	453
SC-SPAE60	230	347	349	421	434
SC-SPAE50	218	345	348	404	443
SC-SPAE40	218	439	461	498	509
SC-PAE100	129	499	499	515	515

with concentrated sulfuric acid at 80 °C for 5 h to give sulfonated monomer SDFBS. Under this mild condition, the sulfonate substitution reaction occurred primarily at the para-position to the ether linkage of DFDE because electronic and steric effects made this position more reactive than other ones. ^1H NMR and ^{13}C NMR (Figure 1) characterizations confirmed the chemical structures of DFDE and SDFBS.

First, hydroquinone and 4,4'-biphenol were used as bisphenol monomer to copolymerize with DCDPS and SDFBS. However, only brittle copolymers with low molecular weight were obtained. To enhance the reactivity of bisphenol monomer and simultaneously ensure the wholly aromatic structure of the copolymer, more reactive DHDPE was selected as bisphenol monomer instead of hydroquinone or 4,4'-biphenol. The preparation of side-chain-type sulfonated poly(arylene ether)s (SC-SPAE) was carried out by K_2CO_3 -mediated nucleophilic polycondensation reaction. As shown in Scheme 2, DHDPE, DCDPS, and the sulfonate monomer SDFBS were copolymerized in tetramethylene sulfone (TMS), and toluene was used to dehydrate the reaction system. The reaction temperature was first controlled at 140 °C to remove the water generated during the bisphenoxide formation, and then increased slowly to 180 °C to accomplish polymerization. The sulfonate degree (DS) of SC-SPAE copolymer was defined as the ratio of the number of sulfonate groups per average repeat unit of copolymer. Because the copolymers were prepared by reacting one mole of bisphenol monomer (i.e., DHDPE) with one mole of bishalide monomer (i.e., DCDPS and DFSDE), the copolymers with different DS could be obtained by adjusting the feed ratio of the sulfonated monomer DFSDE to the unsulfonated monomer DCDPS. SC-SPAEs with relative high DS (0.4–1.0) were synthesized for fabrication of membranes with satisfied proton conductivities. Details of the resulting copolymers such as viscosity, sulfonate degree (DS), and ion exchange capacity (IEC) are listed in Table 1. The viscosity values of the resulting sulfonated copolymers were in the range of 1.76–2.48 dL/g, which indicated the copolymerization had been conducted successfully despite the existence of bulky pendant groups in DFSDE. In addition, tough and ductile membranes could be obtained from these copolymers by solvent-casting method (except for SC-SPAE100, its membrane was not robust), which also confirmed their high molecular weights. All of the

Table 3. Water Uptake and Swelling Ratio of SC-SPAEs

polymer	RT, 24 h				80 °C, 10 h			
	water uptake (%)		swelling ratio (%)		water uptake (%)		swelling ratio (%)	
	acid	sodium	acid	sodium	acid	sodium	acid	sodium
SC-SPAE100	19.3	12.8	8.3	6.6	36.0	19.7	13.6	10
SC-SPAE90	16.1	10.3	7.1	5.9	33.6	18.8	11.6	9.2
SC-SPAE80	13.3	7.4	6.2	3.7	23.4	9.9	9.3	5.2
SC-SPAE70	11.5	6.0	5.4	2.7	18.0	8.5	7.6	3.2
SC-SPAE60	9.3	4.3	2.6	2.5	15.8	7.4	4.5	2.5
SC-SPAE50	7.2	3.9	1.8	1.2	13.5	5.6	3.5	1.2
SC-SPAE40	6.8	3.6	0.9	0.8	10.3	3.7	2.0	0.8
Nafion 117	19.2		13.1		29.4		20.2	

sulfonated copolymers were soluble in high polar aprotic solvents, such as DMSO, NMP, DMAc, and DMF, but insoluble or only became swollen in chloroform or THF.

The chemical structures of SC-SPAEs were confirmed by FT-IR and ^1H NMR spectra. As shown in FT-IR spectra (Figure 2), as compared to unsulfonated SC-PAE (derived from polymerization of DHDPE and DFDE) and PAES (derived from polymerization of DHDPE and DCDPS), SC-SPAE copolymers showed a new characteristic peak at 1034 cm^{-1} assigned to $\text{O}=\text{S}=\text{O}$ stretching vibration of sodium sulfonate groups. The bands at 1150 and 1670 cm^{-1} corresponding to stretching vibrations of the diphenylsulfone and diphenylcarbonyl segments, respectively, were also observed in the spectra of SC-SPAEs. These results confirmed successful introduction of the sulfonated groups onto the polymer side chains. Figure 3 showed the ^1H NMR stacked spectra of SC-SPAE80, SC-SPAE100, PAES, and SC-PAE in the aromatic region. Although the ^1H NMR spectra of SC-SPAE copolymers appeared complex and overlapped to some extent, which made the analysis pretty difficult, the assignment of the each spectrum could be accomplished on the basis of 2D ($\text{H}-\text{H}$ COSY) NMR and by its comparison with fully assigned spectra of PAES and SC-PAE. Aromatic protons located at the electron-rich *ortho*-ether position were strongly shielded, and their signals appeared at low frequency ($6.6\text{--}7.2\text{ ppm}$) area, while the protons located at *para*- or *ortho*-positions of sulfone, carbonyl, and sulfonate groups were deshielded due to their strongly electron-withdrawing effects, and their signals appeared at high frequency area ($7.4\text{--}8.0\text{ ppm}$).

Membrane Formation and Ionic Exchange Capacity. The resulting SC-SPAE copolymers showed good solubility in high polar aprotic solvent, allowing the fabrication of the membranes by solvent casting method. After casting from DMAc solution and subsequently proton-exchanging in $1\text{ M H}_2\text{SO}_4$, tough and transparent acid-form membranes were obtained. The ion exchange capacity values (IEC) of these acid-form membranes were determined by classical acid–base titration (Table 1). The experimental IEC values were in the range from 0.8 to $1.74\text{ mequiv g}^{-1}$, almost the same as the theoretical data derived from monomer feed ratios, which indicated that sodium-form SC-SPAEs had been fully converted to their corresponding acid-form ones after the proton-exchange process. These results also confirmed that the sulfonate content in the obtained SC-SPAE copolymers was well consistent with the feed ratios used in the direct copolymerization.

Thermal Properties of SC-SPAEs. Both thermal properties of SC-SPAE membranes in sodium and acid forms were evaluated by their T_g and T_d data (Table 2) measured by DSC and TGA, respectively. No obvious glass transition could be observed for the acid-form SC-SPAEs in our experiments. The T_g of the sodium-form SC-SPAEs increased from 218 to 254 °C when the DS increased from 0.4 to 1.0 , which were much higher than that of unsulfonated SC-PAE (129 °C). Table

2 gave the 5% and 10% weight loss temperatures of the obtained copolymers. Although SC-SPAEs exhibited much lower T_d than SC-PAE, $T_{d5\%}$ and $T_{d10\%}$ of SC-SPAE were over 300 °C in air, which could satisfy the requirement of thermal stability for the use in PEMFC ($>200\text{ °C}$). Figure 4 presented typical TGA curves for SC-SPAE80 and unsulfonated SC-PAE in air. The SC-SPAE80 exhibited two distinct thermal degradation steps. In acid form and sodium form, the first weight loss step was at about 240 and 340 °C , respectively, associated with the loss of the sulfonate groups. Their second weight loss step started at about 500 °C , close to the decomposition temperature of unsulfonated SC-PAE, indicating that the second step was primarily due to the degradation of the copolymer chains.

Water Uptake and Swelling Ratio. For most proton conductive polymers, water acts as the carrier for proton transportation through the polymer membrane. Adequate hydration of electrolyte membranes is crucial for high proton conductivity. However, water swelling ratio should be also considered because extreme swelling will decrease the dimensional stability and mechanical properties of the polymer films. The water uptake and swelling ratio of the copolymer membranes were determined by measuring the changes in the weight or length of hydrated and dehydrated films at desired temperature (Table 3). The sulfonated copolymers in acid form showed much higher water uptake and swelling ratio than those in sodium form due to hydrogen-bond interactions between water molecules and sulfonic acid groups. For example, at 80 °C , SC-SPAE80 in acid form showed 23.4% water uptake and 9.3% swelling ratio, much higher than those of SC-SPAE80 in sodium form (9.9% water uptake and 5.2% swelling ratio). As expected, water uptake and swelling ratio of the films increased with increasing temperature (Figures 5 and 6) and IEC value (Figure 7). For the membranes with low sulfonate content ($\text{IEC} < 1.36$), the water uptake and swelling ratio increased mildly with increasing temperature. The membranes with high sulfonate content ($\text{IEC} \geq 1.36$) exhibited a sharp increase in water sorption and swelling ratio at high temperature (above 80 °C), attributed to the formation of large and continuous ion network in the sulfonated polymers.^{15a,33}

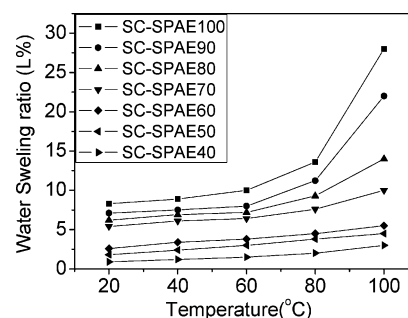


Figure 5. Water swelling ratio of SC-SPAE films as a function of temperature.

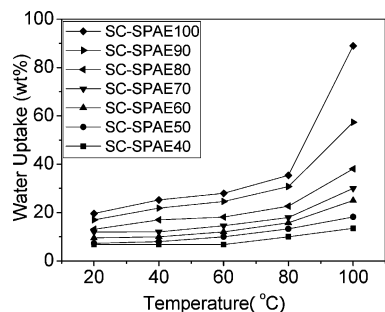


Figure 6. Water uptake of SC-SPAE films as a function of temperature.

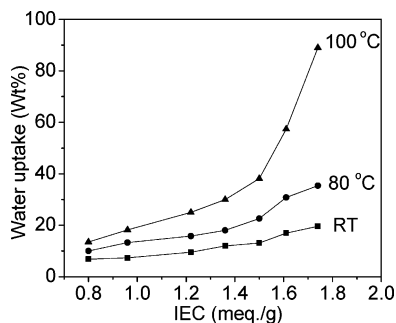


Figure 7. Water uptake versus IEC of the sulfonate polymers SC-SPAEs (acid form) at room temperature (RT), 80 °C, and 100 °C.

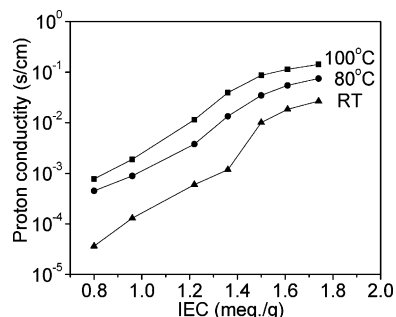


Figure 8. Proton conductivity versus IEC of SC-SPAE films at room temperature (RT), 80 °C, and 100 °C.

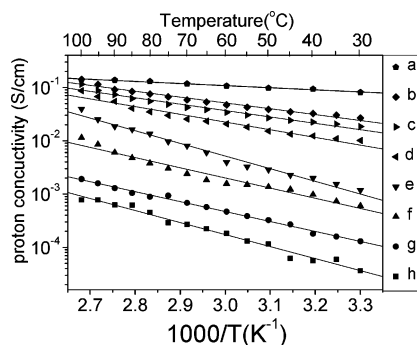


Figure 9. Proton conductivity of SC-SPAE films as a function of temperature (a, Nafion117; b, SC-SPAE100; c, SC-SPAE90; d, SC-SPAE80; e, SC-SPAE70; f, SC-SPAE60; g, SC-SPAE50; h, SC-SPAE40).

At 80 °C, acid-form SC-SPAE90 film (IEC = 1.61 mmol g⁻¹) showed water uptake value (33.6%) and proton conductivity value (0.055 S/cm) similar to those of Nafion 117. However, its water swelling ratio was only 11.6%, about one-half of that of Nafion 117. The water uptake and swelling ratio of these novel SC-SPAEs were also lower than those of other main-chain-type sulfonated poly(arylene ether) with similar IEC value.^{32,34} Even for the homopolymer SC-SPAE100 (polymerized only from DFSDE and DHDPE, IEC = 1.74 mmol g⁻¹),

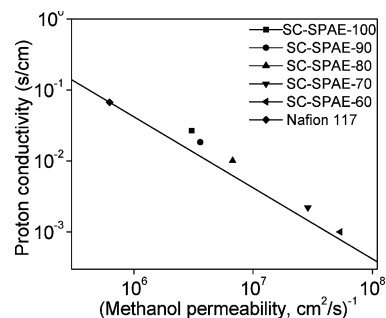


Figure 10. Proton conductivity versus methanol permeability of SC-SPAE films at room temperature.

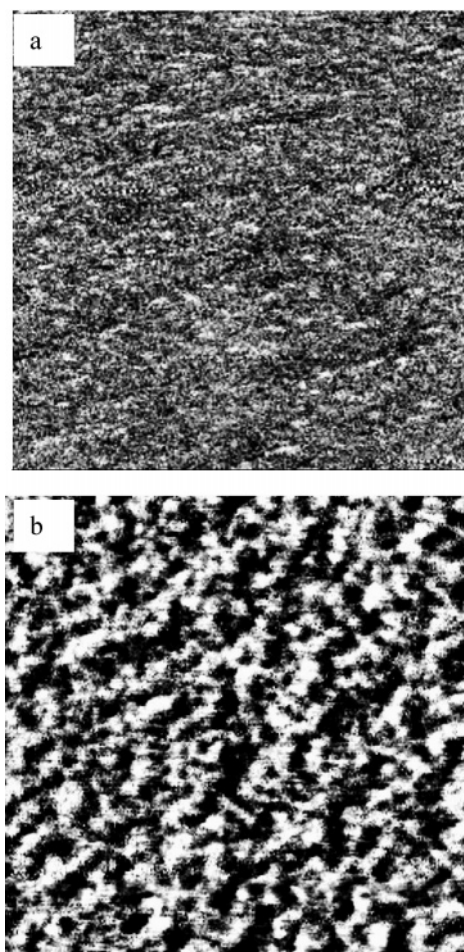


Figure 11. AFM tapping phase images for acid-form SC-SPAE copolymers: (a) SC-SPAE50, (b) SC-SPAE90. Scan boxes are 500 nm × 500 nm, and phase scales are 0–10°.

the water uptake and swelling ratio were only 36.0% and 13.6% at 80 °C (Table 4). SC-SPAE100 showed 89% water uptake at 100 °C, and its swelling ratio was only 28%. The membranes of these side-chain-type copolymers with high IEC value showed suitable water sorption and small dimensional change at the same time. Generally, the existence of short hydrophobic chain between the sulfonic acid groups and polymer main chain favors the nanophase separation in sulfonate polymer,^{17,28a} which will suppress the effect of water sorption on the hydrophobic polymer main chain. As a result, the swelling ratio and water uptake of SC-SPAE films are reduced effectively, similar to the suppressed water uptake of the side-chain sulfonated ionomers with branched structure.^{9g,29d}

Oxidative and Hydrolytic Stability. Oxidative stability of SC-SPAEs membranes was examined by observing their dis-

Table 4. Comparison of Acid-Form SC-SPAEs with Other Sulfonated Poly(arylene ether)s and Nafion 117 in Water Uptake, Swelling Ratio, and Conductivity

polymer	IEC	80 °C		σ (S/cm)		ref
		water uptake (%)	swelling ratio (%)	80 °C	100 °C	
Nafion 117	0.91	29.5	20.2	1.2×10^{-1}	1.4×10^{-1}	this paper
SC-SPAE100	1.81	36.0	13.6	7.5×10^{-2}	1.4×10^{-1}	this paper
SC-SPAE80	1.52	23.4	9.3	3.4×10^{-2}	8.6×10^{-2}	this paper
SPAEEK-6F-50	1.64	68	24	1.1×10^{-1}		33
SPAEEK-6F-60	1.92	157	52	8.0×10^{-2}		33
SPAEEKK-100	1.61	soluble	soluble		5.6×10^{-2}	35
SPAEEKK-90	1.47	87	46.5		3.4×10^{-2}	35

solving behaviors in Fenton's Reagent at 80 °C. The oxidative stability of the membranes decreased with increasing sulfonated degree. SC-SPAE100, SC-SPAE90, and SC-SPAE80 membranes began to dissolve (membrane edges became dim) after 4 h and disappeared after 50 h. However, the membranes of SC-SPAE40, SC-SPAE50, SC-SPAE60, and SC-SPAE70 still remained after 50 h soaking in Fenton's Reagent at 80 °C. These results demonstrated that SC-SPAE membranes have good oxidative stability due to their wholly aromatic structure. The specially designed side-chain-type structure was responsible for the improved oxidative stability because the sulfonation took place only at flexible pendant side chains, and the effect of sulfonic acid groups on the hydrolysis of main chain was greatly minimized accordingly.

The SC-SPAE membranes were also soaked in water at 100 °C for a week to evaluate its hydrolytic stability. As a result, no obvious changes were observed in its appearance or in weight, indicating the excellent hydrolytic stability of the SC-SPAE membranes, which was comparable to that of highly hydrolysis-resistance sulfonated poly(phthalazinone ether ketone) reported by Chen et al. (no change in its appearance and strength after immersing in 100 °C water for about 100 h).³⁶

Proton Conductivities and Methanol Permeability. Proton conductivities of the acid-form SC-SPAE membranes and Nafion 117 were measured at 100% RH in air. The proton conductivity increased with sulfonate content (Figure 8) and temperature (Figure 9). All of the obtained films exhibited reasonable proton conductivity under fully hydrated condition. Even for SC-SPAE40 with IEC value of 0.8 mmol g⁻¹, its proton conductivity reached 10⁻³ S/cm at 100 °C. When the IEC value increased to 1.5 mmol/g (SC-SPAE80), the proton conductivity increased to 10⁻² S/cm at room temperature and increased to 10⁻¹ S/cm at 100 °C, suitable for practical application as PEMs in fuel cell. In case of SC-SPAE90 and SC-SPAE100, the proton conductivity reached 1.2×10^{-1} and 1.4×10^{-1} S/cm at 100 °C, respectively.

From Figure 9, the apparent activation energy of SC-SPAE80 for proton conduction was estimated to be about 25.2 kJ/mol from the asymptotic slope at 30–100 °C, higher than that of Nafion 117 (9.1 kJ/mol), but lower than that of main-chain-type SPEEK with similar IEC value (about 41.0 kJ/mol).³² As discussed above, these copolymers with high proton conductivity showed moderate water uptake and low swelling ratio at high temperature, which endowed them with good dimensional stability. As compared to other main-chain-type sulfonated poly(arylene ether)s, the SC-SPAEs with same IEC value showed much lower water content but similar (as compared SC-SPAE90 with SPAEEK-6F-50³³) or higher proton conductivity (as compared SC-SPAE90 with SPAEEKK-100³⁵). Considering these sulfonated copolymers possessed similar main-chain structure and IEC value, we think the difference of their conductivity mainly results from the position of sulfonate groups in the polymers. Sulfonate groups attached on polymer pendants

could decrease the limitation of main-chain rigidity on the mobility of the sulfonate groups, making the formation of ionic network more readily and thus enhancing the proton conductivity of the ionomers.³⁷ Although the proton conductivities of SC-SPAE membranes were a little lower than that of Nafion 117 at room temperature, the conductivities of SC-SPAE90 and SC-SPAE100 were comparable to that of Nafion117 at high temperature.

However, like other wholly aromatic sulfonated poly(arylene ether), the obtained membranes with high sulfonate content (DS > 0.9) were a little brittle in dry condition due to their wholly aromatic and high rigidity structure. The work on how to decrease their brittleness in dry condition is ongoing in our group and will be reported later.

Membranes intended for direct methanol fuel cell (DMFC) must both possess high proton conductivity and be an effective barrier for methanol crossover from the anode to the cathode compartment. The methanol permeability values for 15 mol/L methanol of SC-SPAE (–100 to 50) at room temperature were in the range of 3.28×10^{-7} to 3.18×10^{-9} cm²/s (Table 1), which is much lower than the value of Nafion 117 of 1.61×10^{-6} cm²/s (data measured in our laboratories). As was previous reported,³⁸ we evaluated the obtained membranes according to a figure that has the logarithm of the proton conductivity as the ordinate and the logarithm of the reciprocal of methanol permeability as the abscissa. Figure 10 shows the relationship of proton and the inverse of methanol permeability of polymeric films. All of the membrane, with low methanol permeability, located on the right-hand side of the line. The SC-SPAE (IEC ≥ 1.36) membranes exhibit high proton conductivity and low methanol permeability and could be promising materials for DMFC applications.

Mechanical Property. The mechanical properties of SC-SPAE70 and 90 membranes have been tested. The samples in the dry state have tensile stress at maximum load of 46.0–30.0 MPa, Young's moduli of 1.85 and 1.45 GPa, and elongation at break of 5.1% and 2.0%. In the wet state, the tensile stress and Young's moduli of the samples decreased. For example, the tensile stress and Young's moduli of SC-SPAE70 decreased to 31 MPa and 1.1 GPa. However, their elongations at break increased to 15.2%, which indicates the samples become more flexible in the wet state.

Morphology. Tapping mode phase images of the acid-form SC-SPAE50 and SC-SPAE90 were recorded under ambient condition on a 500 nm \times 500 nm size scale to investigate the ionic clusters (Figure 11). The dark regions in the images were assigned to a soft structure, corresponding to the hydrophilic sulfonate groups containing water. The bright phases in the images were attributed to a hard structure, corresponding to hydrophobic polymer matrix. For SC-SPAE50, the domains assigned to the hydrophilic ionic cluster were small in size (5–10 nm) and well separated from each other due to its low sulfonate content. Therefore, the membrane showed lower water

uptake and proton conductivity. However, for SC-SPAE90 with higher sulfonate content, the hydrophilic/hydrophobic nanophase separation became more obvious. The hydrophilic ionic domains were large in size (20–30 nm) and became continuous to some extent. Such micro-structure of SC-SPAE90 allows the effective proton transportation via the membrane; therefore, the membrane showed high proton conductivity and low water swelling ratio at the same time.

Conclusions

A series of novel wholly aromatic side-chain-type sulfonated poly(arylene ether) copolymers (SC-SPAE) with different sulfonate degrees were successfully synthesized by direct copolymerization method. The sulfonate content of the copolymers can be readily controlled by adjusting the feed ratio of the sulfonated and unsulfonated monomers. These ionomers possess high molecular weight and can form tough and flexible membranes via solvent casting. Because of their wholly aromatic structures, the membranes present good oxidative, hydrolytic, and thermal stability. The membranes showed both high proton conductivity and good dimensional stability at high temperature due to the introduction of sulfonic acid groups in the side chains. For SC-SPAE90 and SC-SPAE100, their proton conductivities reached 0.1 S/cm at 100 °C, comparable to that of Nafion 117, and their swelling ratios are lower than that of Nafion 117. AFM observations suggested that the copolymer with high sulfonate content showed improved nanophase separation, favorable for the effective proton transportation via the membrane. It is expected that the properties of the membranes can be further improved by rational design of the sulfonated monomer used in the copolymerization.

References and Notes

- (1) Roziere, J.; Jones, D. *J. Annu. Rev. Mater. Res.* **2003**, *33*, 503.
- (2) Hickner, M. A.; Ghassemi, H.; Kim, Y. S.; Einsla, B. R.; McGrath, J. E. *Chem. Rev.* **2004**, *104*, 4587–4612.
- (3) Jannasch, P. *Fuel Cells* **2005**, *5*, 248.
- (4) Wieser, C. *Fuel Cells* **2004**, *4*, 245.
- (5) (a) Ulrich, H. H.; Rafler, G. *Angew. Makromol. Chem.* **1998**, *263*, 71. (b) Alberti, G.; Casciola, M.; Massinelli, L.; Bauer, B. *J. Membr. Sci.* **2001**, *185*, 73.
- (6) (a) Zaidi, S. M. J.; Mikhailenko, S. D.; Robertson, G. P.; Guiver, M. D.; Kaliaguine, S. *J. Membr. Sci.* **2000**, *173*, 17. (b) Kaliaguine, S.; Mikhailenko, S. D.; Wang, K.; Xing, P.; Robertson, G. P.; Guiver, M. D. *Catal. Today* **2003**, *82*, 213. (c) Robertson, G. P.; Mikhailenko, S. D.; Wang, K.; Xing, P.; Guiver, M. D.; Kaliaguine, S. *J. Membr. Sci.* **2003**, *219*, 113. (d) Xing, P.; Robertson, G. P.; Guiver, M. D.; Mikhailenko, S. D.; Wang, K.; Kaliaguine, S. *J. Membr. Sci.* **2004**, *229*, 95.
- (7) (a) Kerres, J.; Ullrich, A.; Meier, F.; Haring, Th. *Solid State Ionics* **1999**, *125*, 243. (b) Daoust, D.; Devaux, J.; Godard, P. *Polym. Int.* **2001**, *50*, 917.
- (8) (a) Nolte, R.; Ledjeff, K.; Bauer, M.; Muelhaupt, R. *J. Membr. Sci.* **1993**, *83*, 211.
- (9) (a) Genies, C.; Mercier, R.; Sillion, B.; Cornet, N.; Gebel, G.; Pineri, M. *Polymer* **2001**, *42*, 359. (b) Guo, X.; Fang, J.; Watari, T.; Tanaka, K.; Kita, H.; Okamoto, K. *Macromolecules* **2002**, *35*, 6707. (c) Guo, X.; Fang, J.; Watari, T.; Tanaka, K.; Kita, H.; Okamoto, K. *Macromolecules* **2002**, *35*, 9022. (d) Miyatake, K.; Zhou, H.; Uchida, H.; Watanabe, M. *Chem. Commun.* **2003**, 368. (e) Miyatake, K.; Asano, N.; Watanabe, M. *J. Polym. Sci., Part A: Polym. Chem.* **2003**, *41*, 3901. (f) Einsla, B. R.; Hong, Y.; Kim, Y. S.; Wang, F.; Gunduz, N.; McGrath, J. E. *J. Polym. Sci., Part A: Polym. Chem.* **2004**, *42*, 862. (g) Miyatake, K.; Zhou, H.; Watanabe, M. *Macromolecules* **2004**, *37*, 4956.
- (10) Zhang, H. B.; Pang, J. H.; Wang, D.; Li, A. Z.; Jiang, Z. H. *J. Membr. Sci.* **2005**, *264*, 56.
- (11) Gao, Y.; Robertson, G. P.; Guiver, M. D.; Mikhailenko, S. D.; Li, X.; Kaliaguine, S. *Macromolecules* **2005**, *38*, 237.
- (12) Jones, D. J.; Roziere, J. *J. Membr. Sci.* **2001**, *185*, 41.
- (13) Roziere, J.; Jones, D. *J. Annu. Rev. Mater. Res.* **2003**, *33*, 503.
- (14) Alberti, G.; Casciola, M.; Massinelli, L.; Bauer, B. *J. Membr. Sci.* **2001**, *185*, 73.
- (15) (a) Wang, F.; Hickner, M.; Kim, Y. S.; Zawodzinski, T. A.; McGrath, J. E. *J. Membr. Sci.* **2002**, *197*, 231. (b) Wang, F.; Hickner, M.; Ji, Q.; Harrison, W.; Mechem, J.; Zawodzinski, T. A.; McGrath, J. E. *Macromol. Symp.* **2001**, *175*, 387.
- (16) Nolte, R.; Ledjeff, K.; Bauer, M.; Muelhaupt, R. *J. Membr. Sci.* **1993**, *83*, 211.
- (17) Kreuer, K. D. *J. Membr. Sci.* **2001**, *185*, 29.
- (18) Kreuer, K. D.; Paddison, S. J.; Spohr, E.; Schuster, M. *Chem. Rev.* **2004**, *104*, 4637.
- (19) Miyatake, K.; Oyaizu, K.; Tsuchida, E.; Hay, A. S. *Macromolecules* **2001**, *34*, 2065.
- (20) Gao, Y.; Robertson, G. P.; Guiver, M. D. *Macromolecules* **2004**, *37*, 18.
- (21) Li, Z.; Ding, J.; Robertson, G. P.; Guiver, M. D. *Macromolecules* **2006**, *39*, 6990.
- (22) (a) Gieselman, M. B.; Reynolds, J. R. *Macromolecules* **1992**, *25*, 4832. (b) Glipa, X.; Haddad, M. El.; Jones, D. J.; Roziere, J. *Solid State Ionics* **1997**, *97*, 323.
- (23) Ghassemi, H.; Ndip, G.; McGrath, J. E. *Polymer* **2004**, *45*, 5855.
- (24) Kobayashi, T.; Rikukawa, M.; Sanui, K.; Ogata, N. *Solid State Ionics* **1998**, *106*, 219.
- (25) Ghassemi, H.; McGrath, J. E. *Polymer* **2004**, *45*, 5847.
- (26) Kerres, J. A. *Fuel Cells* **2005**, *5*, 230.
- (27) (a) Qiu, Z.; Wu, S.; Li, Z.; Zang, S.; Xing, W.; Liu, C. *Macromolecules* **2006**, *39*, 6425. (b) Wu, S.; Qiu, Z.; Zang, S.; Yang, X.; Yang, F.; Li, Z. *Polymer* **2006**, *47*, 6993.
- (28) (a) Lafitte, B.; Karlsson, L. E.; Jannasch, P. *Macromol. Rapid Commun.* **2002**, *23*, 896. (b) Karlsson, L. E.; Jannasch, P. *J. Membr. Sci.* **2004**, *230*, 61. (c) Lafitte, B.; Puchner, M.; Jannasch, P. *Macromol. Rapid Commun.* **2005**, *26*, 1464.
- (29) (a) Yin, Y.; Fang, J. H.; Kita, H.; Okamoto, K. *Chem. Lett.* **2003**, *32*, 4. (b) Asano, N.; Miyatake, K.; Watanabe, M. *Chem. Mater.* **2004**, *16*, 2841. (c) Song, J. M.; Asaoki, N.; Miyatake, K.; Uchida, H.; Watanabe, M. *Chem. Lett.* **2005**, *34*, 7. (d) Zhou, H.; Miyatake, K.; Watanabe, M. *Fuel Cells* **2005**, *5*, 296. (e) Asano, N.; Aoki, M.; Suzuki, S.; Miyatake, K.; Uchida, H.; Watanabe, M. *J. Am. Chem. Soc.* **2006**, *128*, 1762.
- (30) Xing, P.; Robertson, G. P.; Guiver, M. D.; Mikhailenko, S. D.; Kaliaguine, S. *Polymer* **2005**, *46*, 3257.
- (31) Jung, B.; Kim, B. Y.; Yang, J. M. *J. Membr. Sci.* **2004**, *245*, 61.
- (32) Li, L.; Zhang, J.; Wang, Y. *J. Membr. Sci.* **2003**, *226*, 159.
- (33) Xing, P.; Robertson, G. P.; Guiver, M. D.; Mikhailenko, S. D.; Kaliaguine, S. *Macromolecules* **2004**, *37*, 7960.
- (34) (a) Gebel, G.; Moore, R. B. *Macromolecules* **2000**, *33*, 4850. (b) Kim, Y. S.; Hickner, M.; Dong, L.; Pivovar, B.; McGrath, J. E. *J. Membr. Sci.* **2004**, *243*, 317. (c) Sumner, M. J.; Harrison, W. L.; Weyers, R. M.; Kim, Y. S.; McGrath, J. E.; Riffle, J. S.; Brink, A.; Brink, M. H. *J. Membr. Sci.* **2004**, *239*, 199.
- (35) Gao, Y.; Robertson, G. P.; Guiver, M. D.; Mikhailenko, S. D.; Li, X.; Kaliaguine, S. *Macromolecules* **2004**, *37*, 6748.
- (36) Chen, Y. L.; Meng, Y. Z.; Hay, A. Y. *Macromolecules* **2005**, *38*, 3546.
- (37) Spohr, E.; Commer, P.; Kornyshev, A. A. *J. Phys. Chem. B* **2002**, *106*, 10560.
- (38) Pivovar, B. S.; Wang, Y. X.; Cussler, E. L. *J. Membr. Sci.* **1999**, *154*, 155.

MA070080S